



Preparation, Micromorphology and Optical Properties of SPION/Ba₃V₂O₈:Er³⁺, Yb³⁺ Nanocomposites by Microwave-Assisted Metathetic Method

CHANG SUNG LIM

Department of Advanced Materials Science & Engineering, Hanseo University, Seosan 356-706, Republic of Korea

*Corresponding author: Tel/Fax: +82 41 6601445; E-mail: cslim@hanseo.ac.kr

Received: 12 October 2013;

Accepted: 28 February 2014;

Published online: 10 March 2014;

AJC-14917

The nanocomposites of Er³⁺/Yb³⁺ co-doped Ba₃V₂O₈ (Ba₃V₂O₈:Er³⁺/Yb³⁺) with superparamagnetic iron oxide nanoparticles (SPIONs) have been successfully synthesized by microwave-assisted metathetic method followed by heat-treatment. The microstructure exhibited well-defined and homogeneous morphology with the Ba₃V₂O₈:Er³⁺/Yb³⁺ particle size of 1-3 μm and Fe₃O₄ particle size of 100-500 nm. The Fe₃O₄ nanoparticles were self-preferentially crystallized and immobilized on the surface of Ba₃V₂O₈:Er³⁺/Yb³⁺ particles. The synthesized SPION/Ba₃V₂O₈:Er³⁺/Yb³⁺ nanocomposites were characterized by X-ray diffraction, scanning electron microscopy and energy-dispersive X-ray spectroscopy. Other optical properties were also investigated by photoluminescence emission measurements and Raman spectroscopy.

Keywords: Micromorphology, Optical properties, SPION/Ba₃V₂O₈:Er³⁺/Yb³⁺, Microwave-assisted metathetic method.

INTRODUCTION

Superparamagnetic iron oxide nanoparticles (SPIONs) are widely used in various biomedical applications, such as targeted drug delivery and magnetic resonance imaging. It is necessary to constitute a multifunctional nanoplatform by integrating multiple nanoparticle components into a single nanosystem by rational assembly and hybridization techniques. Magnetic-luminescent bifunctional nanocomposites containing the SPIONs incorporated into photoluminescent composites could provide novel characteristics *via* the integration of fluorescent and magnetic properties, offering new potential in a wide range of applications in biomedical systems, such as targeted drugs, diagnostics, therapeutics and bio-imaging¹⁻³.

The metal orthovanadates have been developed to enhance the applications of metal orthovanadate prepared by a range of processes, such as a solid-state reaction^{4,5}, the solution phase metathetic method⁶, the sol-gel⁷, the solid-state metathesis approach⁸, the mechano-chemical method⁹ and the floating zone technique¹⁰. As compared to common methods, the microwave synthesis technique provides such advantages as a short reaction time, small particle size, narrow particle size distribution and it is the high purity method suitable for the preparation of polycrystalline products. The microwave heating is delivered to the surface of the material by radiant and/or convection heating, which is transferred to the bulk of the material *via* conduction. So, the microwave energy is delivered directly to the material through the molecular interactions with

electromagnetic field. Heat can be generated through volumetric heating because microwaves can penetrate the material and supply energy¹¹⁻¹⁴.

The cyclic microwave-assisted metathetic synthesis of materials is a simple and cost-effective method that provides a high yield with an easy scale-up and it is emerging as a viable alternative approach for the synthesis of high-quality novel inorganic materials in short time periods^{15,16}. In this study, the Er³⁺/Yb³⁺ co-doped Ba₃V₂O₈ (Ba₃V₂O₈:Er³⁺/Yb³⁺) and Er³⁺/Yb³⁺ co-doped Ba₃V₂O₈ with SPIONs (SPION/Ba₃V₂O₈:Er³⁺/Yb³⁺) nanocomposites were synthesized by the cyclic microwave-assisted metathetic method followed by heat-treatment. The synthesized Ba₃V₂O₈:Er³⁺/Yb³⁺ and SPION/Ba₃V₂O₈:Er³⁺, Yb³⁺ nanocomposites were characterized by X-ray diffraction (XRD), scanning electron microscopy (SEM) and energy-dispersive X-ray spectroscopy (EDS). Optical properties have been investigated by photoluminescence emission measurements and Raman spectroscopy.

EXPERIMENTAL

Appropriate stoichiometric amounts of BaCl₂·2H₂O, ErCl₃·6H₂O, YbCl₃·6H₂O, Na₃VO₄, 5 nm sized Fe₃O₄ nanoparticles and ethylene glycol of analytic reagent grade were used to prepare the Ba₃V₂O₈:Er³⁺, Yb³⁺ and SPION/Ba₃V₂O₈:Er³⁺, Yb³⁺ compounds. To prepare Ba₃V₂O₈:Er³⁺/Yb³⁺, 0.8 mol % BaCl₂·2H₂O with 0.02 mol % ErCl₃·6H₂O and 0.18 mol % YbCl₃·6H₂O and 1 mol % Na₃VO₄ were dissolved in 30 mL of ethylene glycol. To prepare SPION/Ba₃V₂O₈:Er³⁺, Yb³⁺, 0.2

mol % $\text{BaCl}_2 \cdot 2\text{H}_2\text{O}$ with 0.02 mol % $\text{ErCl}_3 \cdot 6\text{H}_2\text{O}$ and 0.18 mol % $\text{YbCl}_3 \cdot 6\text{H}_2\text{O}$ and 1 mol % Na_3VO_4 with 0.5 mol % Fe_3O_4 were dissolved in 30 mL ethylene glycol. The solutions were mixed and adjusted to pH 9.5 using NaOH. The solutions were stirred at room temperature. Then, the mixtures were transferred into 120 mL Teflon vessels. Each Teflon vessel was placed into a microwave oven operating at the frequency of 2.45 GHz with the maximum output power of 1250 W for 23 min. The working cycle of the microwave-assisted metathetic reaction was controlled precisely between 30 sec on and 30 sec off for 8 min, followed by a further treatment of 30 sec on and 60 sec off for 15 min. Ethylene glycol was evaporated slowly at its boiling point. Ethylene glycol is a polar solvent at its boiling point of 197 °C and it is a good candidate for the microwave process. The resulted powder samples were treated with ultrasonic radiation and washed many times with hot distilled water. The white precipitates were collected and dried at 100 °C in a drying oven. After this, the final products were heat-treated at 600 °C for 3 h.

The phase composition of final powder products formed after the cyclic microwave-assisted metathetic reaction and following heat-treatment was identified using XRD (D/MAX 2200, Rigaku, Japan). The microstructures and surface morphologies of the $\text{Ba}_3\text{V}_2\text{O}_8\text{:Er}^{3+}/\text{Yb}^{3+}$ and $\text{SPION}/\text{Ba}_3\text{V}_2\text{O}_8\text{:Er}^{3+}/\text{Yb}^{3+}$ nanocomposites were observed using SEM/EDS (JSM-5600, JEOL, Japan). Their photoluminescence spectrum was recorded at room temperature using a spectrophotometer (Perkin Elmer LS55, UK). Raman spectroscopy measurements were performed using a LabRam HR (Jobin-Yvon, France) device. The 514.5-nm line of an Ar-ion laser was used as an excitation source and the power on the samples was kept at 0.5 mW.

RESULTS AND DISCUSSION

Fig. 1 shows the XRD pattern of the synthesized $\text{SPION}/\text{Ba}_3\text{V}_2\text{O}_8\text{:Er}^{3+}/\text{Yb}^{3+}$ nanocomposites. All the observed diffraction peaks can be assigned to the trigonal-phase $\text{Ba}_3\text{V}_2\text{O}_8$ (space group R-3m) and Fe_3O_4 , which were in good agreement with the crystallographic data of $\text{Ba}_3\text{V}_2\text{O}_8$ (JCPDS 71-2060) and Fe_3O_4 (JCPDS 19-0629). The diffraction peaks marked with asterisk are related to Fe_3O_4 . The result confirms that the $\text{SPION}/\text{Ba}_3\text{V}_2\text{O}_8\text{:Er}^{3+}, \text{Yb}^{3+}$ nanocomposites can be prepared using the cyclic microwave-assisted metathetic route. The post-synthesis heat-treatment plays an important role in forming well-defined crystallized micromorphology. To achieve such morphology, the $\text{SPION}/\text{Ba}_3\text{V}_2\text{O}_8\text{:Er}^{3+}, \text{Yb}^{3+}$ nanocomposites need to be heated at 600 °C for 3 h. This suggests that the cyclic

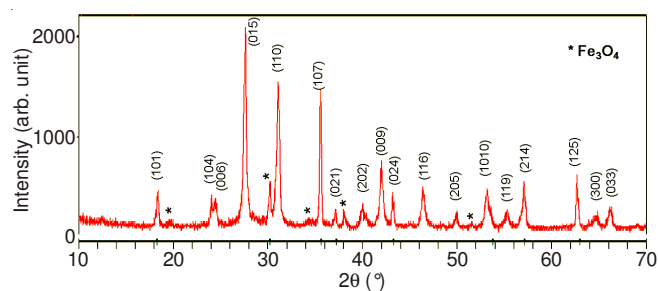


Fig. 1. XRD pattern of the synthesized $\text{SPION}/\text{Ba}_3\text{V}_2\text{O}_8\text{:Er}^{3+}/\text{Yb}^{3+}$ nanocomposites

microwave-assisted metathetic route, in combination with subsequent heat-treatment, is a suitable way for the formation of $\text{SPION}/\text{Ba}_3\text{V}_2\text{O}_8\text{:Er}^{3+}, \text{Yb}^{3+}$ nanocomposites with well developed high-intensity peaks from the at (015), (110) and (107) planes, which are the major peaks of $\text{Ba}_3\text{V}_2\text{O}_8$.

The SEM image of the synthesized (a) $\text{SPION}/\text{Ba}_3\text{V}_2\text{O}_8\text{:Er}^{3+}, \text{Yb}^{3+}$ nanocomposite is shown in Fig. 2. The as-synthesized sample has a well-defined and homogeneous morphology with the particle size of $\text{Ba}_3\text{V}_2\text{O}_8\text{:Er}^{3+}, \text{Yb}^{3+}$ in the range of 1-3 μm and Fe_3O_4 in the range of 100-500 nm, respectively. The Fe_3O_4 nanoparticles were self-preferentially crystallized and immobilized on the surface of big $\text{Ba}_3\text{V}_2\text{O}_8\text{:Er}^{3+}, \text{Yb}^{3+}$ particles. The incorporation of Fe_3O_4 nanoparticles to the $\text{Ba}_3\text{V}_2\text{O}_8\text{:Er}^{3+}, \text{Yb}^{3+}$ compound particles can be successfully achieved using the cyclic microwave-assisted metathetic. The microwave-assisted metathetic reactions, such as $3\text{BaCl}_2 + 2\text{Na}_3\text{VO}_4 \rightarrow \text{Ba}_3\text{V}_2\text{O}_8 + 6\text{NaCl}$, involve the exchange of atomic/ionic species, in which the driving force is the exothermic reaction accompanying the formation of NaCl ¹⁶. The $\text{SPION}/\text{Ba}_3\text{V}_2\text{O}_8\text{:Er}^{3+}, \text{Yb}^{3+}$ nanocomposites were heated rapidly and uniformly by the cyclic microwave-assisted metathetic route. This classifies the method among simple and cost-effective ones and, evidently, the microwave-assisted metathetic technology is able to provide high yields with an easy scale-up as a viable alternative for the rapid synthesis of complex oxide composites¹⁶.

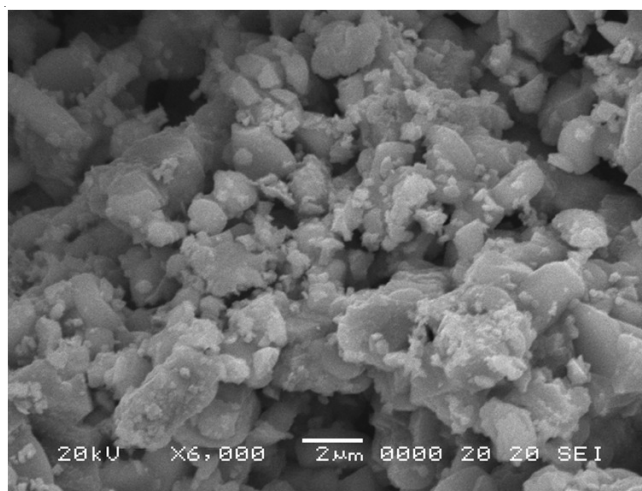


Fig. 2. SEM image of the synthesized (a) $\text{SPION}/\text{Ba}_3\text{V}_2\text{O}_8\text{:Er}^{3+}, \text{Yb}^{3+}$ nanocomposite

The EDS pattern, quantitative compositions, quantitative results and the SEM image of the synthesized $\text{SPION}/\text{Ba}_3\text{V}_2\text{O}_8\text{:Er}^{3+}, \text{Yb}^{3+}$ nanocomposite are presented in Fig. 3. The EDS pattern shown in Fig. 3a displays that the $\text{SPION}/\text{Ba}_3\text{V}_2\text{O}_8\text{:Er}^{3+}, \text{Yb}^{3+}$ sample is composed of Fe, Ba, V, O, Er and Yb with the dominance of Fe, Ba, V, O. The EDS pattern and quantitative compositions in Fig. 3a,b could be well assigned to the $\text{SPION}/\text{Ba}_3\text{V}_2\text{O}_8\text{:Er}^{3+}, \text{Yb}^{3+}$ composite. Thus, the incorporation of Fe_3O_4 nanoparticles to the $\text{SPION}/\text{Ba}_3\text{V}_2\text{O}_8\text{:Er}^{3+}, \text{Yb}^{3+}$ compound particles can be successfully achieved using the cyclic microwave-assisted metathetic. The cyclic microwave-assisted metathetic reactions provide a convenient route for the synthesis of such complex products

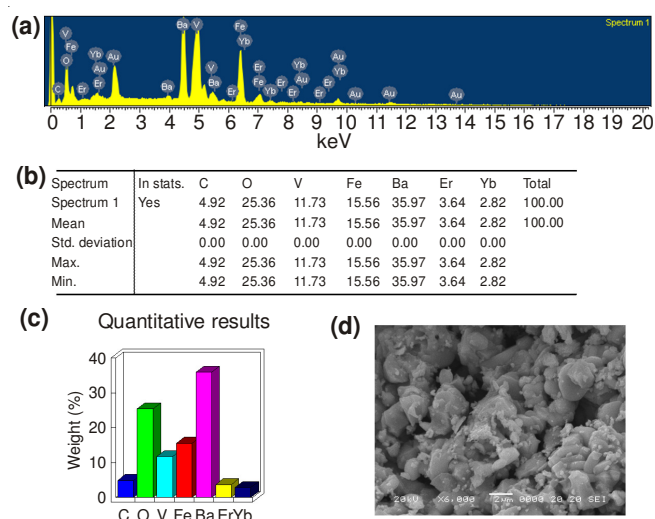


Fig. 3. (a) EDS pattern, (b) quantitative compositions, (c) quantitative results and (d) SEM image of the synthesized SPION/Ba₃V₂O₈:Er³⁺, Yb³⁺ nanocomposites

as SPION/Ba₃V₂O₈:Er³⁺, Yb³⁺ composites. The cyclic microwave-assisted metathetic route provides the exothermic energy to synthesize the bulk of the material uniformly, so that fine particles with controlled morphology can be fabricated in an environmentally friendly manner and without solvent waste generation.

The photoluminescence emission spectrum of the synthesized SPION/Ba₃V₂O₈:Er³⁺, Yb³⁺ nanocomposite excited at 250 nm at room temperature is shown in Fig. 4. It is generally assumed that the measured emission spectrum of metal orthovanadates are due mainly to charge-transfer transitions within the [VO₄]³⁻ complex. With excitation at 250 nm, the spectrum of the nanocomposites exhibit major photoluminescence emissions in the blue wavelength range of 390-430 nm. The emissions of three narrow shoulders at approximately 490, 510 and 530 nm are considered to form by defect structures. The emission spectra of metal orthovanadates are due mainly to charge-transfer transitions within the [VO₄]³⁻ complex. The explanation of the narrow shoulders in Fig. 5 is proposed considering

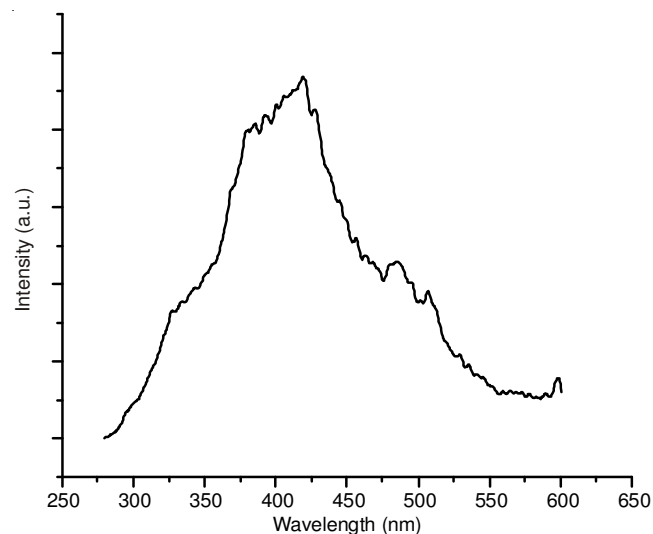


Fig. 4. Photoluminescence emission spectrum of the synthesized SPION/Ba₃V₂O₈:Er³⁺, Yb³⁺ composites excited at 250 nm at room temperature

the Jahn-Teller splitting effect^{17,18} on excited states of [VO₄]³⁻ and anion in the Ba₃V₂O₈. This is similar to that reported by Zhang *et al.*¹⁹. The Jahn-Teller splitting effect essentially determines the emission shape of the Ba₃V₂O₈ particles. The additional emission bands can be interpreted by the existence of Frenkel defect structures (oxygen ion shifted to the interposition with the simultaneous creation of vacancies) in the surface layers of the Ba₃V₂O₈ particles^{20,21}.

Fig. 5 shows the Raman spectra of the synthesized (a) Ba₃V₂O₈ particles and (b) Ba₃V₂O₈:Er³⁺, Yb³⁺ (BVO:ErYb) and SPION/Ba₃V₂O₈:Er³⁺, Yb³⁺ (F-SVO:ErYb) nanocomposites excited by the 514.5 nm line of an Ar-ion laser at 0.5 mW. The Raman modes for the Ba₃V₂O₈ particles in Fig. 5a were detected as ν₁(A_g), ν₃(B_g), ν₃(E_g), ν₄(E_g), ν₄(B_g) and ν₂(B_g) vibrations at 835, 778, 504, 378 and 327 cm⁻¹, the free rotation mode was detected at 168 cm⁻¹ and the external modes were localized at 133 cm⁻¹. The well-resolved sharp peaks for the Ba₃V₂O₈ nanoparticles indicate that the synthesized particles are highly crystallized. The vibration modes in the Raman spectrum of Ba₃V₂O₈ nanoparticles are classified into two groups, internal and external^{22,23}. The internal vibrations are related to the [VO₄]³⁻ molecular group with a stationary mass center. The external vibrations or lattice phonons are associated to the motion of the Ba²⁺ cation and rigid molecular units. The type of cations (Ca²⁺, Sr²⁺, Ba²⁺) can influence on the

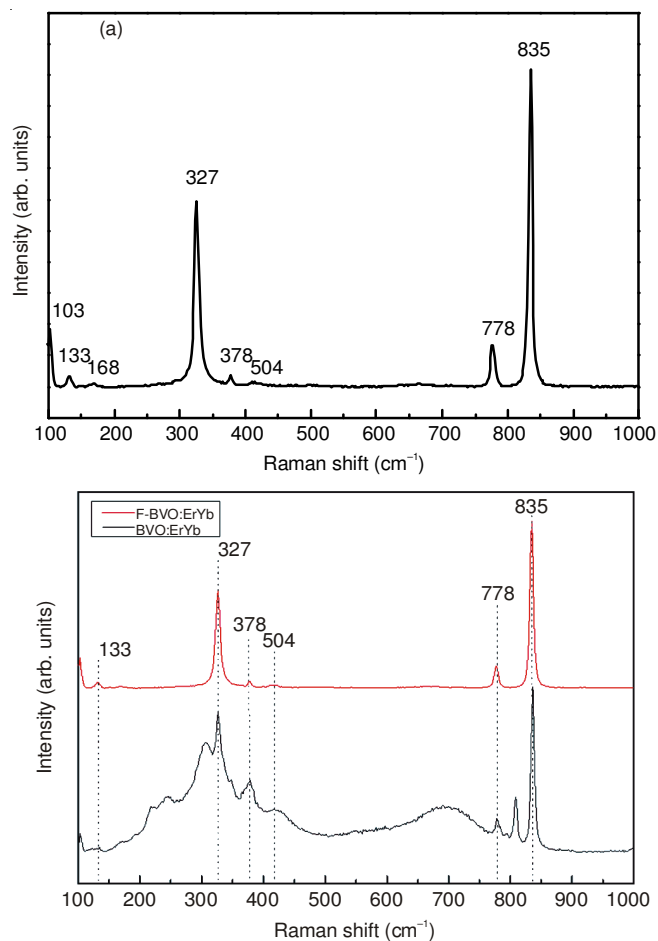


Fig. 5. Raman spectra of the synthesized (a) Ba₃V₂O₈ particles and (b) Ba₃V₂O₈:Er³⁺, Yb³⁺ (BVO:ErYb) and SPION/Ba₃V₂O₈:Er³⁺, Yb³⁺ (F-BVO:ErYb) nanocomposites

Raman modes by changing the size of the crystal unit cell and by covalent cation effect²³. The internal modes for the Ba₃V₂O₈:Er³⁺, Yb³⁺ (BVO:ErYb) and SPION/Ba₃V₂O₈:Er³⁺, Yb³⁺ (F-BVO:ErYb) composites in Fig. 5b were detected as $\nu_1(A_g)$, $\nu_3(B_g)$, $\nu_3(E_g)$, $\nu_4(E_g)$, $\nu_4(B_g)$ and $\nu_2(B_g)$ vibrations at 835, 778, 504, 378 and 327 cm⁻¹, the free rotation mode was detected at 168 cm⁻¹ and the external modes were localized at 133 cm⁻¹. From the comparison in Fig. 5b it can be depicted that the peak positions are practically the same. The internal vibration mode frequencies are dependent on the lattice parameters²³ and the degree of the partially covalent bonding between the cations and molecular ionic group [VO₄]³⁻. Raman spectrum of the synthesized Ba₃V₂O₈:Er³⁺, Yb³⁺ (BVO:ErYb) nanocomposites indicates additional peaks at both higher (810 and 700 cm⁻¹) and lower frequencies (300, 240 and 210 cm⁻¹), which are attributed to the doping ions of Er³⁺ and Yb³⁺²⁴⁻²⁶. It is noted that the Fe₃O₄ particles have no influence on the Raman spectra, while the doping ion of Er³⁺/Yb³⁺ can influence the Raman spectra. Raman spectra proved that the Er³⁺/Yb³⁺ doping ions can influence the structure of the host materials.

Conclusion

The nanocomposites of Er³⁺/Yb³⁺ co-doped Ba₃V₂O₈ (Ba₃V₂O₈:Er³⁺/Yb³⁺) with SPIONs were successfully synthesized by an microwave-assisted metathetic method. The microstructure exhibited a well-defined and homogeneous morphology with the Ba₃V₂O₈:Er³⁺, Yb³⁺ and Fe₃O₄ particle size of 1-3 μ m and 100-500 nm, respectively. The Fe₃O₄ nanoparticles were self-preferentially crystallized and immobilized on the surface of Ba₃V₂O₈:Er³⁺, Yb³⁺ particles. Raman spectrum of the synthesized Ba₃V₂O₈:Er³⁺, Yb³⁺ (BVO:ErYb) nanocomposite indicated additional peaks at both higher (810 and 700 cm⁻¹) and lower frequencies (300, 240 and 210 cm⁻¹), which are attributed to the doping ions of Er³⁺ and Yb³⁺. The Fe₃O₄ particles have no influence on the Raman spectra, while the doping ion of Er³⁺/Yb³⁺ can influence the Raman spectra.

ACKNOWLEDGEMENTS

This study was supported by Basic Science Research Program through the National Research Foundation of Korea

(NRF) funded by the Ministry of Education, Science and Technology (2013-054508).

REFERENCES

1. D. Liu, L. Tong, J. Shi and H. Yang, *J. Alloys Comp.*, **512**, 361 (2012).
2. L. Liu, L. Xiao and H.Y. Zhu, *Chem. Phys. Lett.*, **539-540**, 112 (2012).
3. Q. Wang, X. Yang, L. Yu and H. Yang, *J. Alloys Comp.*, **509**, 9098 (2011).
4. D. Wang, Z. Zou and J. Ye, *Res. Chem. Intermed.*, **31**, 433 (2005).
5. M. Kurzawa and A. Blonska-Tabero, *J. Therm. Anal. Calorim.*, **77**, 17 (2004).
6. P. Parhi and V. Manivannan, *Mater. Res. Bull.*, **43**, 2966 (2008).
7. S.S. Kim, H. Ikuta and M. Wakihara, *Solid State Ion.*, **139**, 57 (2001).
8. P. Parhi, V. Manivannan, S. Kohli and P. Mccurdy, *Bull. Mater. Sci.*, **31**, 885 (2008).
9. V. Manivannan, P. Parhi and J. Howard, *J. Cryst. Growth*, **310**, 2793 (2008).
10. R. Szymczak, M. Baran, J. Fink-Finowicki, B. Krzymanska, P. Aleshkevych, H. Szymczak, S.N. Barilo, G.L. Bychkov and S.V. Shiryaev, *J. Non-Cryst. Solids*, **354**, 4186 (2008).
11. T. Trongtem, A. Phuruangrat and S. Trongtem, *J. Nanopart. Res.*, **12**, 2287 (2010).
12. C.S. Lim, *Mater. Res. Bull.*, **47**, 4220 (2012).
13. C.S. Lim, *Asian J. Chem.*, **25**, 63 (2013).
14. S. Das, A.K. Mukhopadhyay, S. Datta and D. Basu, *Bull. Mater. Sci.*, **32**, 1 (2009).
15. C.S. Lim, *J. Lumin.*, **132**, 1774 (2012).
16. C.S. Lim, *Mater. Chem. Phys.*, **131**, 714 (2012).
17. Y. Toyozawa, M. Inoue, *J. Phys. Soc. Jpn.*, **21**, 1663 (1966).
18. E.G. Reut, *Izv. Akad. Nauk SSSR, Ser. Fiz.*, **43**, 1186 (1979).
19. Y. Zhang, N.A.W. Holzwarth and R.T. Williams, *Phys. Rev. B*, **57**, 12738 (1998).
20. J. Van Tol, *Mol. Phys.*, **88**, 803 (1996).
21. V.B. Mikhailik, H. Kraus, D. Wahl and M.S. Mykhaylyk, *Phys. Status Solid B*, **242**, R17 (2005).
22. T.T. Basiev, A.A. Sobol, Y.K. Voronko and P.G. Zverev, *Opt. Mater.*, **15**, 205 (2000).
23. T.T. Basiev, A.A. Sobol, P.G. Zverev, L.I. Ivleva, V.V. Osiko and R.C. Powell, *Opt. Mater.*, **11**, 307 (1997).
24. C.S. Lim, *Mater. Chem. Phys.*, **140**, 154 (2013).
25. V.V. Atuchin, V.G. Grossman, S.V. Adichtchev, N.V. Surovtsev, T.A. Gavrilova and B.G. Bazarov, *Opt. Mater.*, **34**, 812 (2012).
26. C.S. Lim, *Mater. Res. Bull.*, **48**, 3805 (2013).